Volume 1 | Number 1 | Jan 2013 | Pages 1–100

ChemComm

Chemical Communications
www.rsc.org/chemcomm

ROYAL SOCIETY OF CHEMISTRY

ROYAL SOCIETY OF CHEMISTRY

www.rsc.org/chemcomm

Graphical abstract

Highly sensitive and selective colorimetric detection of glucose was performed using peroxidase-like activity of NiTe TNWs with excellent magnetic performance.

ARTICLE TYPE

Novel magnetic nickel telluride nanowires decorated with thorn: Synthesis and their intrinsic peroxidase-like activity for detection of glucose

Lijuan Wan,[a,b] **Jinhuai Liu**[b] **and Xing-Jiu Huang*** [b]

The magnetic nickel telluride with thorny nanostructure is directly synthesized for the first time via a hydrothermal method. They were used to detect H_2O_2 and glucose with a limit of detection of 25 nM (linear range =0.1~0.5 μM), and 0.42 μM (linear range =1~50 μM), respectively.

Hydrogen peroxide (H_2O_2) is produced in chemical, biological, pharmaceutical, clinical, and environmental processes.[1,2] It is popular to detect H_2O_2 and glucose using the traditional optical[3,4] and electrochemical[5] approaches in which most assays use natural peroxidases. Obviously, these methods have practical drawbacks such as lack of sensitivity, time-consuming fabrication procedures and need for expensive reagents.

Nanomaterials (NMs) such as Fe_3O_4,[6] Au @ Pt,[7] and graphene[8] have been used to detect H_2O_2 for their catalytic activity is similar to that of natural peroxidases. For example, NMs could catalyze the oxidation of the peroxidase substrates such as 2, 20-azino-bis (3-ethylbenzothiazoline-6-sulfonic acid) diammonium salt (ABTS)[9,10] and 3,3',5,5'-tetramethylbenzidine (TMB)[11] using the catalytic activity of the released metal ions. NMs meet the requirements of low cost, ease of preparation, stability, and sensitivity.

Semiconducting tellurides are widely used in various fields due to the properties of electrochemistry,[12] photoluminescence[13] and magnetism.[14] Typical magnetic tellurides such as FeTe,[15] CoTe[16] and NiTe[17] are regarded as environment friendly NMs could be further recycled and reused. Roy et al. reported FeTe nanorods were used as enzyme mimics to detect glucose[9] and mercury[18] in blood.

In this study, novel magnetic nickel telluride nanowires decorated with much thorn were prepared for the first time through a hydrothermal method. In order to evaluate the practical potential of the as-obtained NiTe thorny nanowires (TNWs), we investigated the peroxidase-like property by catalyzing the oxidation of ABTS with H_2O_2. A colorimetric detection system constructed with glucose oxidase (GO_x), NiTe TNWs and ABTS was used for the determination of glucose. As we know, biological applications of CoTe and NiTe are few reported.

The diameter and length of the as-synthesized NiTe TNWs were estimated from their corresponding SEM and TEM images to be ~45 nm and ~5 μm, respectively (Fig. 1(a,b)). From the TEM image, we see clearly much thorn around the nanowires.

The diffraction peaks of the XRD patterns (Fig. 1c) can be indexed to a rhombohedral crystal structure (JCPDS No. 65-3665). The detection of Te and Ni in the EDS spectrum (Fig. 1d) further confirms the formation of NiTe. It is necessary to point out that the signal of Sc element originates from the sample bar of TEM device and does not affect our results.
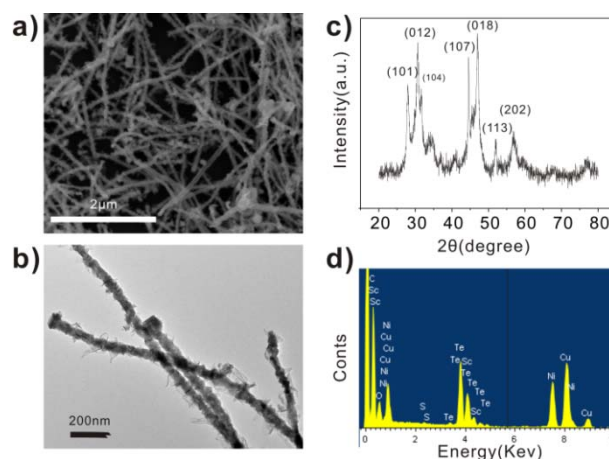
Fig. 1 Characterization of the as-synthesized NiTe TNWs. (a, b) SEM and TEM images, (c, d) XRD and EDS spectrum, respectively.

The saturation magnetization (Ms), remanent magnetization (Mr), and coercivity (Hc) values of NiTe TNWs measured at room temperature are 2.5, 0.61 emu/g, and 140 Oe, respectively (Fig. 2). So, it is believed that the as-prepared NiTe with relatively high coercivity could be utilized as recycle and reuse materials. To our knowledge, the hysteresis loops for NiTe were not reported in previous literatures yet. NiTe NWs were formed through a coreduction reaction in alkaline solution (supporting information).

We determined the peroxidase-like activity of NiTe TNWs that catalyze the reaction of H_2O_2 with substrate ABTS (Eqn (1)). The reaction mechanism follows the oxidation reaction of ABTS into the radical-cation $ABTS^{+ \cdot}$ in the presence of H_2O_2. Bi et al. explained the reaction process by using magnetic grapheme oxide-supported hemin as peroxidase probe to detect sensitively

thiols in extracts of cancer cells.[19] Because the amount of the colored oxidized product of ABTS (λmax = 418 nm) produced is proportional to the concentration of H_2O_2 present in the solution, the concentration of H_2O_2 can be determined by recording the absorbance at 418 nm of the solution according to Beer's law.[9]

$$H_2O_2 + ABTS \xrightarrow{\text{NiTe TNWs}} \text{Oxidized ABTS} + 2H_2O \quad (1)$$
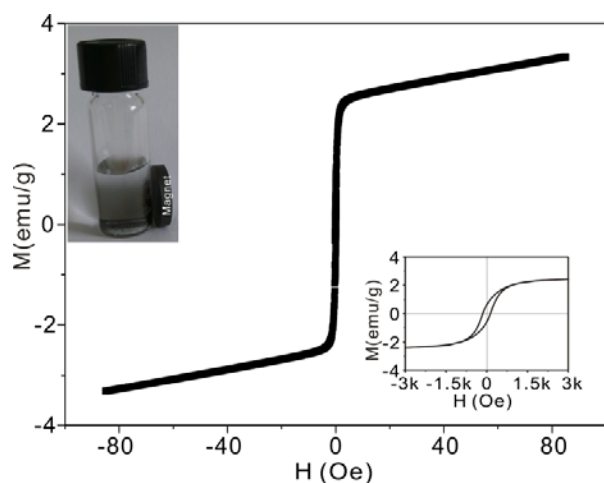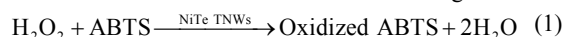

Fig. 2 Magnetic hysteresis curves measured at room temperature for NiTe TNWs. The right inset shows local enlarged hysteresis loop with an applied field between -3k and 3k Oe. The left inset is a photograph.

The as-prepared NiTe TNWs provided about 24-fold absorbance value at 418 nm of that in the absence of the NiTe TNWs (Fig. 3a). Under the conditions, the catalytic activity of NiTe TNWs is 3 times higher than that of the commercial NiTe powder. The morphology and size of commercial NiTe samples were given in Fig. S1. In order to exclude other possibilities, absorption spectra of solution containing NiTe TNWs in the presence of ABTS or H_2O_2 are also shown in Fig. 3a.

The catalytic activity is related to the solution pH, reaction temperature, and kinds of solvent.[11,20] Fig. S2 (ESI†) shows the response curves in acetate buffer solutions (0.2 M) containing 100 μM H_2O_2 over a pH range of 3.0~8.0 at 30℃. Decomposition of H_2O_2 occurs rapidly at a pH higher than 5.0, leading to loss of its oxidation activity toward ABTS. Therein, insufficient amount of Ni^{2+} ions available in the solution also accounts for low activity. In the presence of the NiTe TNWs, the absorbance increased when the reaction temperatures were raised from 20 to 60 ℃. We plotted the differential absorbance (DA) values against reaction temperature in the range 20~60 ℃ (Fig. S3, ESI†), in which DA = A418 nm (NiTe TNWs) - A418 nm (Blank), the maximum value of DA for the NiTe TNWs occurred at 30℃.

According to the proportional relationship between catalytic activity and amount of released Ni^{2+}, it is speculated that the released Ni^{2+} from NiTe TNWs reach a maximum value at 30℃. The peroxidase-like activities of NiTe TNWs in acetonitrile and isopropanol organic solvents were studied. The maximal absorbance appeared blue shift at ~396 nm in acetonitrile solvent (Fig. S4a, ESI†) compared with 418 nm in acetate buffer solution. The time-dependent UV absorption spectra indicated that the catalytic oxidation of ABTS by NiTe TNWs followed the

Michaelis–Menten behavior (Fig.S4b, ESI†). Additionally, there was no absorbance peak in isopropanol solvent. From Fig. S5, it can be obtained that the values of K_m and V_{max} are 0.011 mM and 4.27×10^{-8} M s^{-1}, respectively, suggesting that NiTe TNWs have higher affinity toward ABTS and comparable reaction velocity.
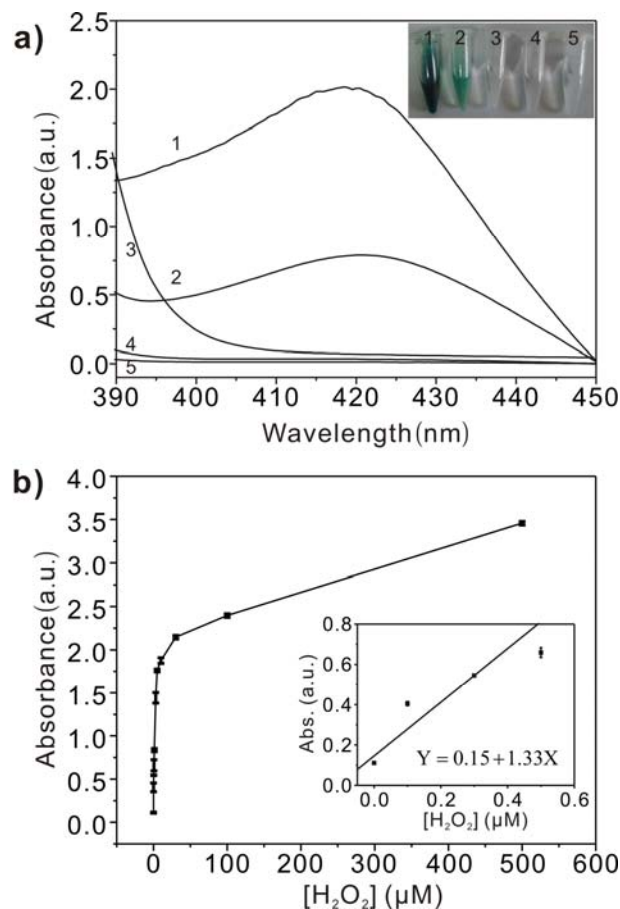

Fig. 3 (a) Absorption spectra of solution containg (1) NiTe TNWs + ABTS + H_2O_2 (2) commercial NiTe + ABTS + H_2O_2 (3) ABTS (4) NiTe TNWs + ABTS and (5) NiTe TNWs + H_2O_2. Inset: photograph. Concentrations: ABTS (60 mM), H_2O_2 (100 μM), commercial NiTe (2.0 mg·ml^{-1}), and NiTe TNWs (2.0 mg·ml^{-1}). Acetate buffer: (0.2 M, pH 4.0). (b) A dose–response curve for H_2O_2 detection when using NiTe TNWs. Inset: linearity of absorbance (Y) against H_2O_2 concentration (X) ranging over 0.1~ 0.5 μM.

The optimum parameters of pH and temperature are 4.0 and 30, respectively. Under the optimized conditions, we investigated a linear relationship between the absorbance (Y) and H_2O_2 concentration (X) range of 0.1~500 μM and obtained a limit of detection of 25 nM with the regression equation of Y=0.15+1.33X (R^2 = 0.97) (Fig. 3b).

Combination of the catalytic reaction shown in Eqn (1) with the glucose catalytic reaction by GO_x (Eqn (2)), colorimetric detection of glucose can be realized. The H_2O_2 produced in Eqn (2) reacted subsequently with ABTS that was catalyzed by NiTe TNWs as shown in Eqn (1). The absorbance against the concentration of glucose is linear (inset to Fig. 4a) in the range

1~50 μm with equation of Y=0.44+0.02X (R^2=0.97); and a limit of detection of 0.42 μM is found. Control experiments were carried out to test the specificity of the developed system by using 5 mM fructose, lactose, maltose, dopamine and ascorbic acid all instead of glucose (Fig. 4b).

$$O_2 + Glu\cos e \xrightarrow{\quad GO_x \quad} H_2O_2 + Gluconic\ acid \quad (2)$$

In contrast to electrochemical biosensors and colorimetric sensors constructed with PtPd-Fe$_3$O$_4$ dumbbell,[21,22] NiTe TNWs system shows comparable sensitivity, selectivity and acceptable recyclability (Fig.S6, ESI†).
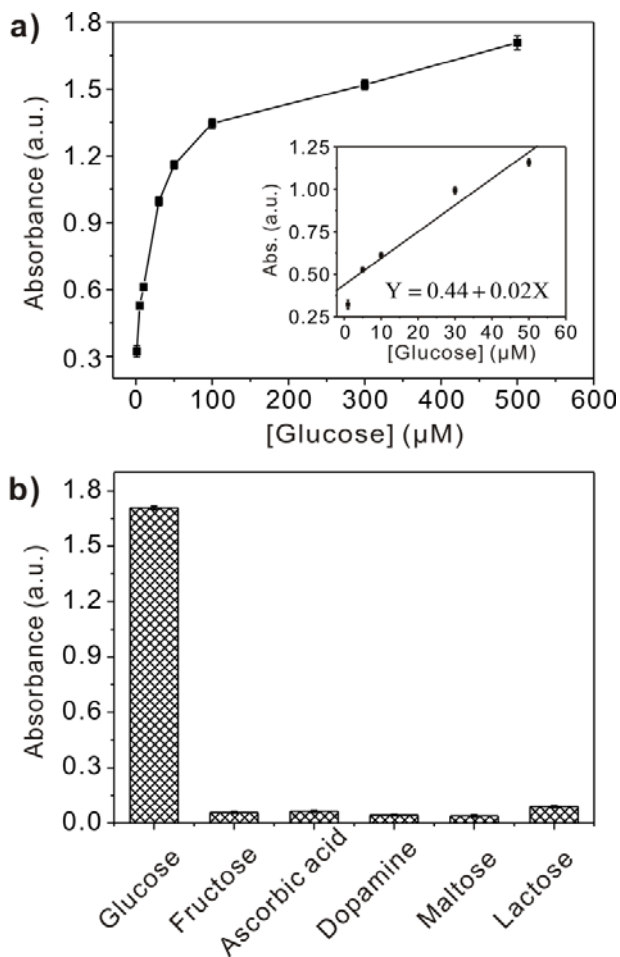

Fig. 4 (a) A dose-response curve for the detection of glucose in a system including GO$_x$ and NiTe TNWs. Inset: linearity of absorbance (Y) against a glucose concentration (X) range of 1~50 μM. (b) Specificity analysis of the glucose detection. Concentrations of solutes are 500 μM for glucose and 5 mM for the other common interfering species. Other conditions are the same as in Fig. 3a.

In summary, the magnetic NiTe TNWs with novel nanostructure were directly synthesized for the first time through the hydrothermal method. The as-prepared NiTe TNWs have a higher catalytic activity toward H$_2$O$_2$-mediated ABTS reaction than those of commercial NiTe powder. The catalytic activity of NiTe TNWs is related with pH, temperature and kinds of solvent. Under the optimized conditions (pH 4.0, 30℃) using GO$_x$ and NiTe TNWs system, the assay provided relatively high sensitivity and selectivity for the detection of glucose.

Notes and references

[a] Hefei Teacher's College, Hefei, 230061, P.R. China
[b] Research Center for Biomimetic Functional Materials and Sensing Devices, Institute of Intelligent Machines, Chinese Academy of Sciences, Hefei, 230031, P.R. China. Fax: +86 551 5592420; Tel: +86 551 5591142; E-mail: xingjiuhuang@iim.ac.cn
† Electronic Supplementary Information (ESI) available: Experimental details, chemical reaction of NiTe NWs, SEM image of the commercial NiTe powder, pH-Temp response curves, time-dependent UV absorption spectra, Michaelis-Menten constant. See DOI: 10.1039/b000000x/

1 M.-J. Song, S.W. Hwang and D. Whang, *Talanta*, 2010, **80**, 1648.
2 M. Giorgio, M. Trinei, E. Migliaccio and P.G. Pelicci, *Nat. Rev. Mol. Cell. Biol.*, 2007, **8**, 722.
3 A. McNeillie, D.H. Brown, W.E. Smith, M. Gibson and L. Watson, *J. Chem. Soc., Dalton Trans.*, 1980, 767.
4 Z. Rosenzweig and R. Kopelman, *Anal. Chem.*, 1996, **68**, 1408.
5 G.Y. Shi, J.X. Lu, F. Xu, H.G. Zhou, L.T. Jin and J.Y. Jin, *Anal. Chim. Acta.*, 2000, **413**, 131.
6 H. Wei and E. Wang, *Anal. Chem.*, 2008, **80**, 2250.
7 J.B. Liu, X.N. Hu, S. Hou, T. Wen, W.Q. Liu, X. Zhu, J.J. Yin and X.C. Wu, *Sens. Actuators, B*, 2012, **166**, 708.
8 X.M. Chen, X.T. Tian, B.Y. Su, Z.Y. Huang, X. Chen and M. Oyama, *Dalton T*, 2014, **43**, 7449.
9 P. Roy, Z.H. Lin, C.T. Liang and H.T. Chang, *Chem. Commun.*, 2012, **48**, 4079.
10 D.M. Hushpulian, V.A. Fechina, S.V. Kazakov, I.Y. Sakharov and I.G. Gazaryan, *Biochemistry-Moscow+*, 2003, **68**, 1006.
11 N. Li, Y. Yan, B.Y. Xia, J.Y. Wang and X. Wang, *Biosens. Bioelectron.*, 2014, **54**, 521.
12 Q. Li, H.B. Li, H.Q. Fan, W.Q. Jie, M.M. Xu, H.R. Wang, J. Cryst. Growth. 372 (2013) 175-179.
13 J. Suthagar, N.J.S. Kissinger, M. Balasubramaniam and K. Perumal, *Sci. China Technol. Sc.*, 2011, **54**, 52.
14 K. Palandage, G.W. Fernando, K. Fang and A.N. Kocharian, *J. Mater.Sci.* 2012, **47**, 7671.
15 J. Kumar, P.K. Ahluwalia, S. Auluck and V.P.S. Awana, *Aip. Conf. Proc.*, 2012, **1447**, 893.
16 N. Umeyama, M. Tokumoto, S. Yagi, M. Tomura, K. Tokiwa, T. Fujii, R. Toda, N. Miyakawa and S.I. Ikeda, *Jpn. J. Appl. Phys.*, 2012, 51.
17 H.M. Helmy, C. Ballhaus, J. Berndt, C. Bocrath and C. Wohlgemuth-Ueberwasser, *Contrib. Mineral. Petr.*, 2007, **153**, 577.
18 P. Roy, Z.H. Lin, C.T. Liang and H.T. Chang, *J. Hazard. Mater.*, 2012, **243**, 286.
19 S. Bi, T.T. Zhao, X.Q. Jia and P. He, Biosens. *Bioelectron.*, 2014, **57**, 110.
20 T. Takashima, K. Hashimoto and R. Nakamura, *J. Amer. Chem. Soc.*, 2011, **134**, 1519.
21 Z.J. Yang, Y. Tang, J. Li, Y.C. Zhang and X.Y. Hu, *Biosens. Bioelectron.*, 2014, **54**, 528.
22 X.L. Sun, S.J. Guo, C.S. Chung, W.L. Zhu and S.H. Sun, *Adv. Mater.*, 2013, **25**, 132.

ChemComm Accepted Manuscript